STOPPING OF ENERGETIC RADIOACTIVE IONS USING CYCLOTRON PRINCIPLES*

F. Marti, Y. Batygin, G. Bollen, C. M. Campbell, S. Chouhan, C. Guénaut, D. Lawton, D. J. Morrissey, J. Ottarson, G. Keith Pang, S. Schwarz, B. Sherrill, A. Zeller,

NSCL, East Lansing, Michigan 48824, U.S.A.

Abstract

The Cyclotron Gas Stopper is a device being studied at the NSCL to stop radioactive ions produced by projectile fragmentation at high energies (~ 140 MeV/u) and to convert them into low-energy ion beams (keV). The low-energy beams of singly or doubly charged ions can be used directly for precision experiments or be reaccelerated for nuclear reaction and spectroscopic studies.

INTRODUCTION

The stopping of the fast ion beams in gas to provide low energy beams is an integral part of the low-energy physics program at the NSCL. The conversion of relativistic fragments into low-energy beams is important because it allows the rare isotopes produced by projectile fragmentation to be used in experiments at low energies (stopped beams). At present the NSCL operates a low energy program centered on precision mass measurements of exotic nuclei and is beginning a program in laser spectroscopy. The mass measurement program has produced dramatic results in the first few years of operation and continues to be able to measure nuclei at the limits of stability but the present system has reached a technical limit that has begun to hamper the experimental program.

The basic principle of gas stopping is simple: after appropriate slowing down of the fast fragments in solid degraders the ions are finally stopped in a chamber with helium gas. As the ions remain singly or doubly-charged due to the high ionization potential of helium, they can be guided out of the gas cell using electric and/or magnetic fields and gas flow and then converted into a low-emittance low-energy ion beam by means of RF ion guiding techniques. The difficulties lie in the details of the ion transport from the region of high ionization caused by the stopping process through a beam extraction orifice into the ion guides.

Gas stopping devices for fast fragments have been built and extensively studied at MSU [1, 2, 3] and at other present-generation (low-power) fragmentation facilities in Japan [4, 5] and in Germany [6, 7]. Although these devices have been used successfully for experimental programs they all fall short of fulfilling the requirements indicated above. We propose to use a new gas-stopping concept, the cyclotron gas stopper [8, 9]. This device is based on a gas-filled sector cyclotron magnet combined with radiofrequency ion guiding techniques in the extraction region. We believe that the new technique can be applied to a large range of isotopes without introducing significant losses of efficiency.

GAS STOPPING CONCEPTS

Several groups from around the world are presently working on projects to stop ion beams in gas filled chambers from both projectile fragmentation processes [3, 4, 5] and low energy reactions [10, 11] based, in part, on the long history of IGISOL devices [12, 13 and references therein]. All of the groups use elongated gas-filled chambers that are equipped with electrodes to transport the stopped ions to a small orifice by means of static and/or RF electric fields. The efficient collection of fragmentation beams with large momentum distributions from the production reaction requires ion-optical range compression of the secondary-beam momentum distribution [14] in order to keep the gas cell size reasonable and to minimize ion extraction times.

Gas cells exist at the NSCL and at RIKEN for general operation with projectile fragment beams and one test was carried out with a 280 MeV/u beam at GSI. At RIKEN substantial R&D work has been performed [4, 5] on stopping very light ion beams at energies of approximately 80 MeV/u and the first successful experiments with ^{8}Be have recently been reported. A slightly smaller gas catcher built by a collaboration headed by the ANL group [15] was tested with radioactive sources before it was tested at low beam rates with neutron deficient chromium isotopes at about 280 MeV/u but no detailed results are available. The NSCL gas stopping system has seen the largest number of experimental tests and the widest range of extracted beams (more than four years of operation and thirty experimental runs). Significant expertise and a solid understanding of the performance and limitations of linear gas stoppers have been gained from these tests.

GAS STOPPING ISSUES

Momentum spread and momentum compression

Stopping energetic secondary beams within a limited-size gaseous helium target is a challenging task due the momentum distribution of the secondary beam and range straggling. The total momentum spread of a given secondary beam produced by projectile fragmentation is on the order of a few percent and is determined by the differential energy loss and energy straggling in the production target, the achromatic wedge used for beam purification, and by the reaction mechanism itself. In

order to be stopped in the gas cell the beam has to be first slowed down with solid degraders. This will increase the momentum spread further. Ion-optical range compression of the secondary-beam momentum distribution [16, 17] is required in order to keep the gas cell size reasonable and to also minimize ion extraction times.

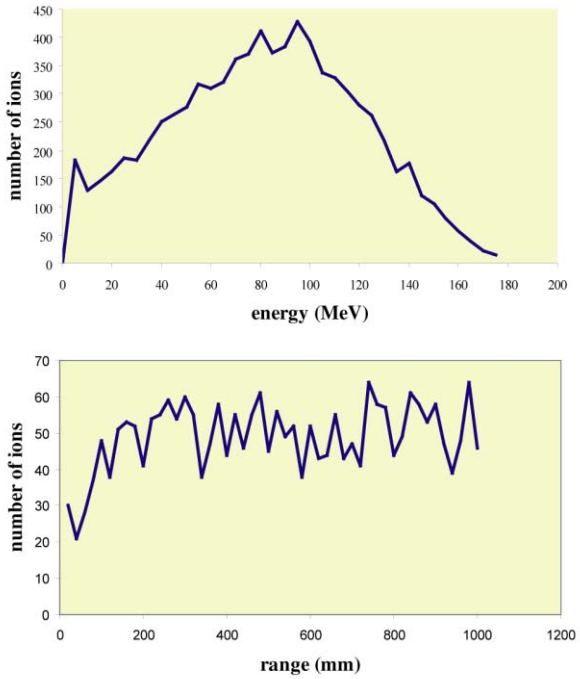

Figure 1: Energy distribution (top) of ^{14}O ions after traversing a Si degrader, emerging at energies around 90 MeV. Distribution of stopped ions along the linear gas cell (bottom). Calculated with SRIM assuming a 1 m long cell operating at 200 mbar helium.

Stopping

Linear gas cells for projectile fragments are presently operated at target effective thickness of less than 10 mg/cm^2. For medium-mass secondary beams (A>60) with energies of a few tens of MeV/u, after passing through a momentum compression stage, such a target thickness is sufficient to achieve a stopping efficiency close to 100 %. The stopping of lighter beams is more challenging. This is due to the large longitudinal range straggling of light ions inside the stopping gas, easily exceeding the length of the stopping volume of the gas cell. With the 50 cm long NSCL gas cell the efficiency for stopping Ca ions is about 50% if a helium pressure of 1 bar is used. With the RIKEN gas cell, nearly 2 meters long and operated at a pressure of 100 mb, only 15% of the incoming Be ions are typically stopped [4]. Employing much larger linear gas cells or much higher pressures is impractical and would also result in longer extraction times. Gas cells for low-energy beams are typically operated at target thicknesses of less than 0.01 bar.m helium to stop medium-mass beams with very good efficiency. This target thickness is about 2 orders of magnitude lower than that required for the stopping of beams from projectile fragmentation.

As an illustration, the results of a simulation of a 1 meter long linear gas cell (200 mbar helium) are shown in Figure 1. The ions were assumed to be produced in a projectile fragmentation facility at the optimum energies with zero energy spread when arriving at the final degrader. A Si degrader was introduced to slow the ions to energies around 90 MeV. The energy distribution of the ions when entering the cell is shown on top and the distribution of stopped ions at the bottom. The large energy straggling observed on the top graph explains why only 12% of the ions stopped in the cell, 19% stopped in the degrader before entering the cell and 69% hit the end wall. Increasing the degrader thickness will reduce the ions that hit the end wall, but will also increase the ions lost inside the degrader. Increasing the pressure in the cell would increase the fraction of the ions stopped in the chamber, but this pressure will create difficulties for the proposed RF carpets proposed to guide the ions out of the chamber. High pressures will make it difficult to sustain the electric fields needed to keep the ions of interest away from the chamber walls.

Beam extraction and extraction times

The extraction of the stopped ions from the gas cells normally is based on either pure static fields or a combination of static and RF fields. The average extraction time out of the systems is determined by the gas pressure, the length of the system, and the maximum electric field that can be applied without creating discharges in the helium gas. For stopping high-energy fragment beams (100 MeV/u) in the mid-mass range the gas cell target "thickness" needs to be about p.L=0.5 bar m of helium gas as discussed above. The typical electric field strength obtained for guiding the ions towards the exit of the gas cell are of the order of E=10 V/cm. Using a typical reduced ion mobility of K=20 cm^2/(Vs) results in an extraction time for an ion starting at the entrance window of the gas cell operated at room temperature of textract = p.L/(K p/p0)/E = 250 ms. Assuming a constant electric drift field in the gas cell this leads to an average extraction time of 125 ms. Extraction times of this order pose a limitation on the shortest half-life of the rare isotope to be studied. Lowering the gas pressure would result in shorter extraction times but with a penalty in stopping efficiency. For light, not too short-lived ions an increase in pressure could be desirable, in order to improve the stopping efficiency, if the half-lives are long enough. However, an increase of the gas pressure will drastically reduce the effectiveness of the RF carpet. This is because the effective force, which is generated by the RF-fields and which prevents the ions from touching the electrodes, decreases quadratically with the gas pressure [4].

In contrast to high-energy gas cells, the extraction times from low-energy gas cells are typically in the order of 10 ms. This is due to their small size and the low pressure with which they can be operated.

Charge exchange and neutralization

During the slowing down process the ions undergo charge changes until they finally stop as singly charged or doubly charged ions, depending on their ionization potential. Remaining charged allows them to be transported in and extracted out of the gas cell by means of electric forces. In linear gas cells the exact knowledge of the evolution of the average charge state as a function of the path is not critical. A topic of present discussions is the possible effect of neutralization during this stopping process. More studies are required.

Gas purity

Coming to rest and still spending tens or even hundreds of milliseconds in the helium gas, the stopped rare isotope ions have a chance to undergo molecular reactions. The reactions can happen with the helium gas and with gas impurities and have been observed both in low-energy and high-energy gas cells. The formation of molecular radioactive ions can lead to the formation of molecular ions with a variety of masses and lead to an effective ion loss. It can also be an advantage since it allows one to minimize the presence of beam contamination by shifting the desired rare isotope ion into a "molecular sideband". This technique has been used quite extensively at LEBIT, see [18, 19].

A serious issue is the creation of stable molecular ion beams via charge exchange of gas impurities with the helium ions created during the stopping process. This effect is strongly amplified in high-energy gas cells as compared to low-energy cells for the following reasons. Typically, energies in the range of a few tens of MeV to about one hundred MeV have to be dissipated in the stopping process. With 42 eV required for the formation of an He-ion electron pair, this leads to the creation of 10^6 or more of such ion pairs per stopped rare isotope ion. Impurities at the 2-ppb level at a total helium pressure of 1 bar leads to a charge exchange time constants of $\tau < 20$ ms. With standard gas purification techniques such a low impurity level is difficult to achieve inside the gas cell. As a consequence, if $t_{extract} >> \tau$ all He ions will undergo charge exchange.

Rate limitation due to space-charge effects

The results from systematic studies show a systematic decrease of the efficiency with increasing beam rate. The reduction in efficiency is caused by the ionization of the helium gas during the stopping process of the incoming ions. Since the electrons are removed very quickly the remaining positive charge of the helium ions has to be considered. This positive space charge pushes the desired ions towards the walls of the gas cell and counteracts the voltages applied to drift the ions toward the extraction region of the gas cell. These effects are discussed in [20] and a comprehensive comparison of the extraction efficiency from different gas cell systems for high and low energy beams has been given in [21].

Experimentally observed extraction efficiencies for the NSCL high-energy gas cell system have been compared with the result of particle-in-cell simulations and good agreement is found. Similarly, efficiencies observed for the RIKEN gas cell are well explained by calculations with an analytical model [5]. All results obtained with high-energy beams indicate that, without additional measures, the capability of linear gas cells to extract stopped radioactive ions without a loss in efficiency is well below a rate of 10^5/s. The space charge effects can be mitigated if the helium ions can be removed from the gas cells while the stopped ions are still transported along the gas cell wall toward the extraction orifice. This separation is in principle possible with radiofrequency carpets [4], which can be operated such that an unstable motion is achieved for the helium ions He^+ and He_2^+ and a stable motion for desired ions with masses well above A=8. This mass separation will work as long as the electric field created by the space charge close to the wall is smaller than the opposed effective electric field created by the RF carpet. RF carpets and related RF funnels have been used in the extraction region of the gas cells but no tests with high-energy beams have been performed using carpets installed at the sidewalls of linear gas cells. Nevertheless, it is expected that the beam rate capability of linear gas cells for heavier beams could be increased considerably with this technique. It should be noted that the mass separation and removal of the helium ions will only work if the gas purity is such that the helium ions do not charge exchange with heavier gas impurities before they are lost at the RF carpet wall.

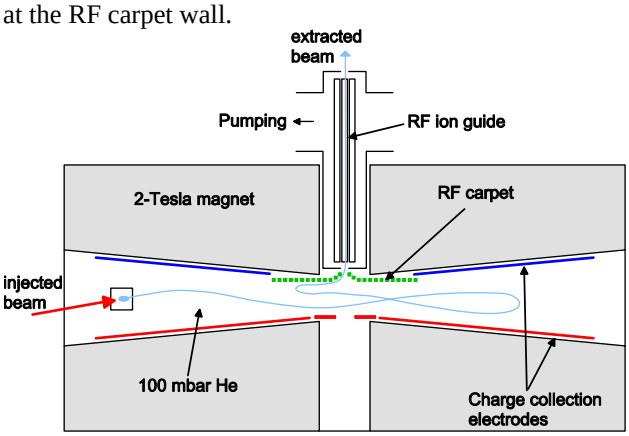

Figure 2: Main components of the Cyclotron Stopper.

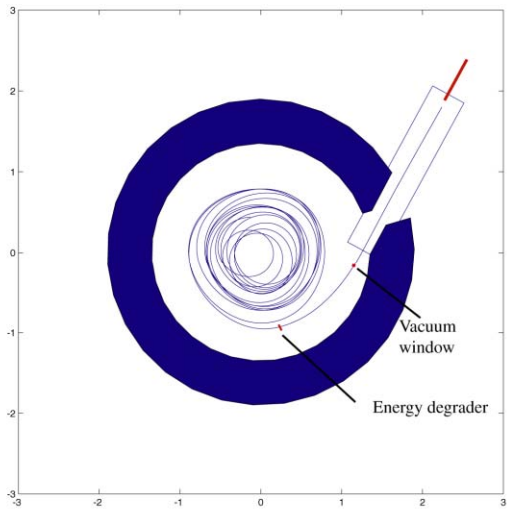

Figure 3: Plot of a 62.7 MeV/u ^{79}Br ion injected in the cyclotron stopper.

CYCLOTRON STOPPER

Origins

The cyclotron gas stopper concept is not new, as gas-filled cyclotrons have been successfully used to stop antiprotons, pions and muons [22, 23]; Katayama et al. have proposed a related scheme [24] to stop light ions and new plans for a cyclotron stopper have been made for RIBF at RIKEN [25]. The concept and the results of first simulations have been discussed in [9]. The focusing properties of a cyclotron-type magnet are used to confine the ions in the radial and axial dimensions during the deceleration process and the ionization is distributed along a much longer path as compared to "conventional" linear gas cells. Figure 2 shows a schematic cross section of such a cyclotron gas stopper. The device consists of a cyclotron magnet and a gas-filled vacuum chamber with charge collection electrodes (for the primary helium ions) close to the pole faces. The fast-fragment beam is injected tangentially into the system and passes through a solid degrader with a thickness adjusted such that the degraded beam follows an inwards spiraling motion caused by the magnetic field and the energy loss in the gas. This process is illustrated in Figure 3, which shows a typical beam trajectory in such a system. The final transport of the ions to the extraction orifice on the central axis uses an RF carpet [24, 4]. Once on the axis, an RF quadrupole ion guide is used to transport the ions through a differential pumping system in the yoke of the magnet.

Magnet design

A conceptual drawing of the mechanical layout of the cyclotron stopper being studied is shown in Figure 4.
The system will use a vertically oriented iron-dominated superconducting magnet with a maximum field strength of approximately 2.5 Tesla. It was found that such an orientation best matches the properties of most beams after momentum compression. Furthermore, the vertical orientation allows the entry path through the (perpendicular) magnetic stray field of the magnet to be carried out at high energy and for the exit path at low energy to be minimized. As shown in Figure 4, the magnet will be constructed such that one half of the yoke can be moved to allow access to the internal components. Penetrations in the yoke needed for beam injection and extraction as well as for chamber support and instrumentation will be arranged in a symmetric pattern.

The inner vacuum chamber will form the volume in which the ions are slowed down and stopped. The stopping chamber in its present design has a radius of approximately 100 cm and an inner height of approximately 10 cm, the beam injection radius is 95 cm. In order to simplify ion injection and to avoid the need to reposition the degrader, the rigidity of all beams injected into the system is fixed at 2.6 Tm. The stopping chamber will be equipped with sets of segmented ionization collection plates and a central RF carpet for the extraction of the stopped secondary ions. The chamber will be cryogenically cooled in order to provide ultra-high vacuum conditions and ensure high purity of the stopping gas inside the chamber.

The fast ion beam will enter the cyclotron gas stopper through an evacuated injection channel, and, after passing through a thin beam window, enter the stopping chamber and pass through an adjustable radial beam degrader. The degrader thickness will be adjusted such that the exiting ion beam has a rigidity of 1.6 Tm, forcing the ions on an inward spiral trajectory.

Once the secondary ions have slowed down and reached the central region a combination of electrostatic and RF fields produced by sets of electrodes and an RF carpet will be used to guide the stopped ions towards the center of the RF carpet. They leave the stopping chamber through an orifice on the central axis. A linear RFQ ion guide system will transport the ions through a differential pumping system into high vacuum. An electrostatic acceleration system will be used outside the yoke to increase the ion energy to a fixed value in the range of 30 - 60 keV for further transport.

The design of the magnetic field is such that it avoids crossing the $\nu_r = 2\ \nu_z$ resonance except close to the center of the magnet. Given the large off centering of the orbits (as shown in Fig. 3) this resonance could produce significant beam blowup.

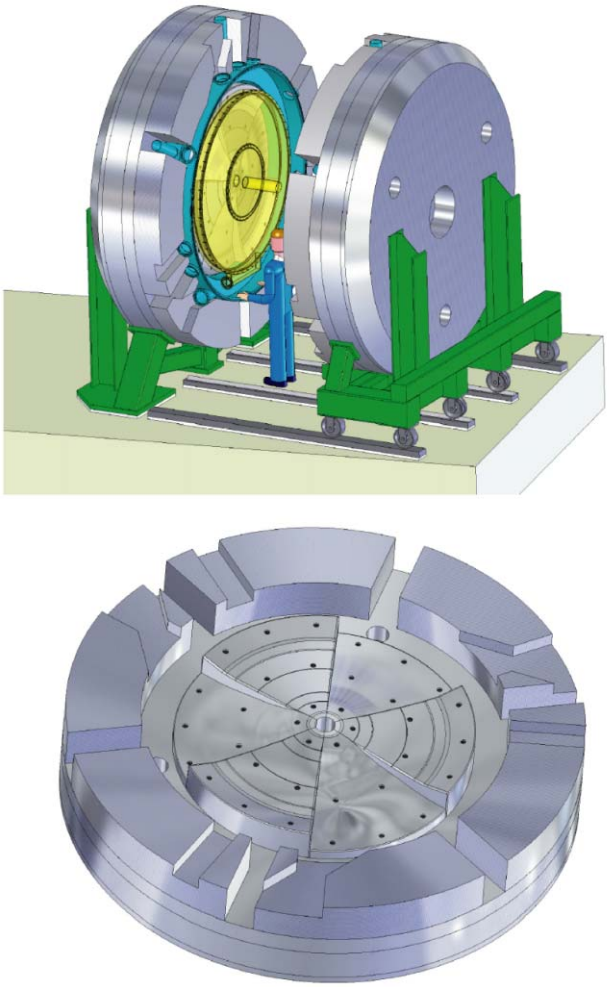

Figure 4: Conceptual design of the cyclotron stopper. The magnet opens in the middle to have access to the beam chamber.

Figure 5 shows the magnetic field in the cyclotron stopper. It is a three-sector magnet. The sectors increase the vertical focusing and simplify the injection.

Simulations

Two computer codes have been developed in parallel to calculate the beam behavior in the cyclotron stopper. This effort has allowed us to test different approaches to several of the physical effects included in the simulations.

The magnetic field has been calculated from 3D TOSCA (Vector Fields) models including all relevant steel penetrations.

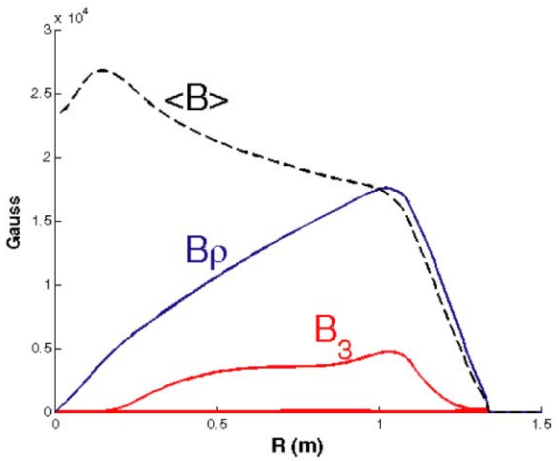

Figure 5: Magnetic field in the cyclotron stopper, showing the average field <B>, Bρ, and the third harmonic component in the median plane.

Energy loss in the cyclotron gas stopper occurs when the ions pass through the beam window, the final degrader and in the stopping gas itself. A version of ATIMA [26] is used to model the beam interaction in solids. It provides the energy loss, the energy-loss straggling and the angular straggling of the ions after passing through the beam window and the degrader. For the energy loss Stopping and Range Tables (SRT) are calculated with SRIM for the different ion species in helium. Below energies of 100 eV the stopping power is described by a viscous drag force obtained from the mobility of ions in helium. The range straggling due to the interaction with the gas is considered but it is typically small compared to that caused by the energy spread of the secondary beam entering the cyclotron stopper.

Angular scattering due to collisions in the gas was not included in the early simulations [9] but was found to be an important process needed to account for possible losses during the end of the stopping path. Two different approaches have been implemented in both simulation codes. The first approach is based on the work on small angle multiple scattering by Sigmund et al. [27]. In the cyclotron stopper simulations the stopping path is divided into layers of thin gas targets with a thickness normally given by the distance between charge changing collisions. After passing a layer the ion direction is randomly changed according to the expected multiple scattering distribution obtained from a parameterization of the Sigmund distributions [27]. The second, more microscopic approach follows a suggestion by Amsel [28] and is based on scattering in single collisions, using an empirical formula for the differential scattering cross sections. Agreement within a factor of 2 is observed and the larger predictions are used for the performance evaluation.

In the early simulations [9] formulas and data from the charge exchange cross sections in [29] were used to determine cross sections and the average charge state of the ions. In the subsequent, more detailed study of the

cyclotron gas stopper concept, a comparison with existing cross section data in light gases at energies above one MeV/u showed that the charge changing cross sections used in [9] were too large by more than an order of magnitude.

For comparison with the linear gas cell results shown in Figure 1 (where only 12% of the ions stopped in the cell), Figure 6 shows the position of the stopped ions from a simulation in the cyclotron stopper of a ^{14}O beam at a pressure of 200 mbar and transverse emittances of 570 π and 1700 π mm mrad. 60% of the injected ions stopped in a radius of less than 20 cm from the center hole. The major loss mechanism is axial losses (30%). The advantages over the linear gas cell discussed above in Figure 1 seem clear in this mass range.

Work continues in the evaluation of the efficiencies of extracting the ions once they have stopped. The inclusion of the RF carpet and space charge forces in the simulations as well as experimental demonstration of the RF carpet parameter limitations are the major activities at the present time.

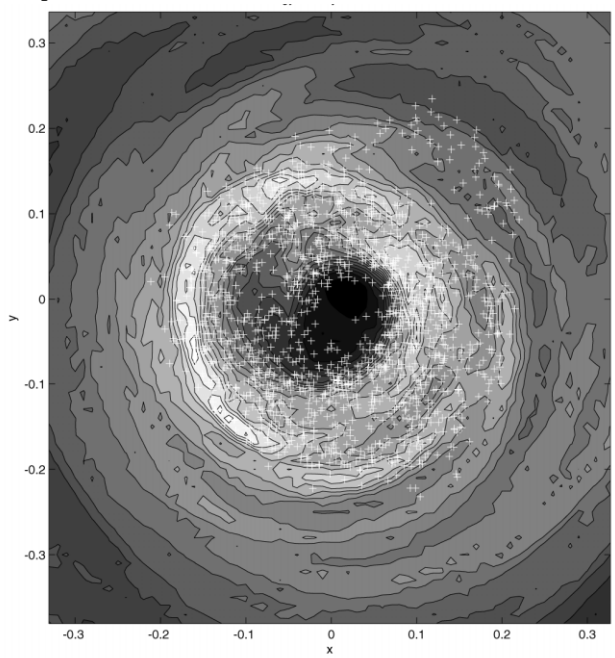

Figure 6: Results from a simulation of the stopping of ^{14}O ions. The crosses indicate the position of the stopped ions. The dimensions are in meters.

REFERENCES

[1] L. Weissman, et al., Nucl. Instr. Meth. A522 (2004) 212.
[2] L. Weissman, et al., Nucl. Instr. Meth. A531 (2004) 416.
[3] L. Weissman, et al., Nucl. Instr. Meth. A540 (2005) 245.
[4] M. Wada, et al., Nucl. Instr. Meth. B204 (2003) 570.
[5] A. Takamine, et al., Rev. Sci. Instrum. 76 (2005) 103503.
[6] C. Scheidenberger, et al., Nucl. Instr. Meth. B204 (2003) 119.
[7] M. Maier, et al., GSI Annual Report 2006, p. 41.
[8] I. Katayama, et al., Hyperfine Int. 115 (1998) 165.
[9] G. Bollen, et al., NIM A550 (2005) 27.
[10] G. Sikler, et al., Nucl. Instr. Meth. B204 (2003) 482.
[11] G. Savard, et al., Nucl. Instr. Meth. B204 (2003) 582.
[12] P. Dendooven, Nucl. Instr. Meth. B126 (2003) 182.
[13] B. Tordoff, et al., Nucl. Instr. Meth. B252 (2006) 347.
[14] H. Weick, et al. Nucl. Instr. Meth. B164-165 (2000) 168.
[15] W. Trimble, et al., Nucl. Phys. A746 (2004) 415c.
[16] H. Weick et al., Nucl. Instr. and Meth. B 164-165 (2000) 168.
[17] C. Scheidenberger et al., Nucl. Instr. and Meth. B 204 (2003) 119.
[18] P. Schury et al., Phys. Rev. C 75 (2007) 055801.
[19]R. Ringle et al., Phys. Rev. C 75 (2007) 055503.
[20]M. Huyse et al., Nucl. Instr. and Meth. B 187 (2002) 535.
[21] D.J. Morrissey, RNB7 proceedings.
[22] L.M. Simons, Physica Scripta T22 (1988) 90.
[23] L.M. Simons, Hyperfine Interactions 81 (1993) 253.
[24] I. Katayama et al., Hyperfine Interactions 115 (1998) 165.
[25] M. Wada, RIKEN, private communication.
[26] J.P. Rozet, C. Stiphan, D. Vemhet, Nucl. Instr. Meth. B107 (1996) 67.
[27] P. Sigmund and K.B. Winterbon, Nucl. Instr. Meth. 119 (1974) 541.
[28] G. Amsel, G. Battistig A. L'Hoir, Nucl. Instr. Meth. B201 (2003) 325.
[29] H.-D. Betz, Charge States and Charge-Changing Cross Sections of Fast Heavy Ions, Rev. Mod. Phys., 44, 465 (1972).